Research paper

Quantification of mRNA encoding cytokines and chemokines and assessment of ciliary function in canine tracheal epithelium during infection with canine respiratory coronavirus (CRCoV)

Simon L. Priestnall [*], Judy A. Mitchell, Harriet W. Brooks, Joe Brownlie, Kerstin Erles

Department of Pathology and Infectious Diseases, The Royal Veterinary College, Hawkshead Lane, Hatfield, Hertfordshire AL9 7TA, UK

ABSTRACT

One of the first lines of defence against viral infection is the innate immune response and the induction of antiviral type I interferons (IFNs). However some viruses, including the group 2 coronaviruses, have evolved mechanisms to overcome or circumvent the host antiviral response. Canine respiratory coronavirus (CRCoV) has previously been shown to have a widespread international presence and has been implicated in outbreaks of canine infectious respiratory disease (CIRD). This study aimed to quantify pro-inflammatory cytokine mRNAs following infection of canine air-interface tracheal cultures with CRCoV. Within this system, immunohistochemistry identified ciliated epithelial and goblet cells as positive for CRCoV, identical to naturally infected cases, thus the data obtained would be fully transferable to the situation *in vivo*. An assay of ciliary function was used to assess potential effects of CRCoV on the mucociliary system. CRCoV was shown to reduce the mRNA levels of the pro-inflammatory cytokines TNF-α and IL-6 and the chemokine IL-8 during the 72 h post-inoculation. The mechanism for this is unknown, however the suppression of a key antiviral strategy during a period of physiologic and immunological stress, such as on entry to a kennel, could potentially predispose a dog to further pathogenic challenge and the development of respiratory disease.

© 2008 Elsevier B.V. All rights reserved.

1. Introduction

Canine respiratory coronavirus (CRCoV) has recently been identified in the respiratory tract of dogs (Erles et al., 2003). CRCoV is a group 2 coronavirus and is genetically most closely related to bovine coronavirus (BCoV). The virus appears to be particularly prevalent in housed populations and within 3 weeks of entry to a kennel, dogs develop antibodies to the virus (Erles et al., 2003). Serological evidence of the virus exists in three continents (Decaro et al., 2007; Kaneshima et al., 2006; Priestnall et al., 2006, 2007), however little is known regarding the pathogenesis of the infection and the possible role of the virus in the canine infectious respiratory disease (CIRD) complex.

To gain further insight into the pathogenesis of CRCoV an infection model is required. Whilst *in vivo* models provide the optimum research tool for viral pathogenesis studies, they are not always feasible or necessary. The ideal *in vitro* model for the study of host-pathogen interactions in the respiratory system would resemble, as closely as possible, the physiologic conditions *in vivo*.

Traditionally, organ cultures involving respiratory tissues have been submerged in medium and thus lacked the air-mucosal interface present *in vivo*. Jackson et al. pioneered the development of respiratory organ cultures with an air-interface using human nasal turbinates (Jackson et al., 1996). Such cultures have a number of

advantages over submerged culture systems including; the presence of all cell types, intact mucociliary clearance and the interaction of the pathogen with the mucus layer and ciliated surface as in vivo.

Using an air-interface system for the culture of turbinate mucosa to model rhinovirus infection, Jang et al. demonstrated that after 7 days of culture the mucosae did not show significant deterioration whilst PCR evidence of rhinoviral infection was recorded (Jang et al., 2005). The authors concluded that such a culture system provided a safe, reliable and physiologically relevant in vitro model for the study of the actions of viruses on the respiratory mucosa.

Structural damage to the respiratory epithelium and abnormal ciliary function are the visible signs of viral infection. However, during airway inflammation, cytokines present at inflammatory sites can be key components in disturbance of the epithelium and persistence of inflammatory reactions. Cytokines can directly or indirectly alter the mucociliary apparatus by affecting ciliary beating or mucus secretion, predisposing to further and more serious viral or bacterial infection.

The primary line of defence against viral infection requires IFN-β production in virus-infected cells, followed by establishment of antiviral functions through activation of the IFN-JAK/STAT signal transduction pathway (Okabayashi et al., 2006). Respiratory epithelial cells also have the ability to synthesize and release pro-inflammatory cytokines, e.g. IL-1β, IL-6 and TNF-α and chemokines, e.g. IL-8 following viral infection (Adachi et al., 1997; Adler et al., 1994; Becker et al., 1993; Brydon et al., 2005).

Viral infection and pro-inflammatory cytokine production stimulate the infiltration of inflammatory cells to the respiratory epithelium. The induction of epithelial chemokines, e.g. IL-8 may also be a primary event triggering increased airway reactivity in acute viral infection (Kazachkov et al., 2002). Production of TNF-α or IL-1 during virus infection may occur either directly or indirectly, for example as a result of cellular damage or via induction of other cytokines. TNF-α has been shown to stimulate mucus glycoprotein secretion by airway epithelial cells within 1 h of exposure (Adler et al., 1994). TNF-α, IL-1β, IL-6 and IL-8 can also affect ciliary beat frequency indirectly through the increased synthesis of endothelin by tracheal epithelial cells (Adler et al., 1994). Quantitative PCR has previously been used to demonstrate significantly increased transcription of IL-6, TNF-α and a number of other pro-inflammatory and immunomodulatory cytokines/chemokines in epithelium infected with feline herpesvirus type-1 (FHV-1), suggesting a previously unknown role for FHV-1 in feline chronic nasal discharge (Johnson and Maggs, 2005).

This study aimed to examine the innate immune response and ciliary function of the canine tracheal epithelium following infection with CRCoV. An in vitro model system using canine air-interface tracheal cultures was developed for this purpose. CRCoV-infected cells were demonstrated using immunohistochemistry and the functional consequences of CRCoV infection were assessed by quantification of cytokine mRNAs and measurement of ciliary function.

2. Materials and methods

2.1. Tracheal cultures

2.1.1. Tissue collection

Dogs were received from a UK re-homing centre having been euthanized due to behavioural concerns and unsuitability to re-home. The whole trachea, from larynx to carina, was aseptically removed at necropsy within 2–3 h of death. The trachea was washed briefly in sterile PBS, then washed twice for 1 h at 37 °C in Dulbecco's modified Eagle's medium (DMEM) containing 2 mM L-glutamine, 50 μg gentamycin mL^{-1}, 100 U penicillin mL^{-1}, 100 μg streptomycin mL^{-1} and 2.5 μg amphotericin B mL^{-1} (Sigma, Poole).

2.1.2. Culture setup and maintenance

Cultures were assembled in a similar manner to that described previously (Anderton et al., 2004). 10 mm^3 3% agarose (Promega, Southampton) cubes (in PBS) were placed into the centre of each well of 6-well cell culture plates (BD Falcon, Oxford) containing DMEM with supplements (Section 2.1.1). 15 mm^2 sterile filter paper squares (Whatman no. 1) were placed onto the surface of the agarose. Following washing, the tracheal ligament was removed and the trachea was sectioned into 10 mm^2 pieces. These pieces were positioned, epithelium uppermost, onto the agar plugs and incubated for up to 120 h at 37 °C, 5% CO_2 and 96–99% RH.

The viability of each trachea was assessed by measuring the ciliary function after 24 h in culture, using a latex bead clearance assay (Section 2.6). Tracheas with >25% of cultures failing to clear beads (score of ≤1) were regarded as non-viable and discarded.

2.1.3. Culture contamination screening

Individual tracheal culture pieces were screened prior to culture setup for respiratory viruses (by PCR) and daily for bacterial contaminants (by culture). Tracheal cultures were discarded if bacterial growth occurred within 72 h (blood agar) or 120 h (mycoplasmas). PCR assays for the detection of canine adenovirus type 2 (CAV-2), canine herpesvirus (CHV), canine parainfluenza virus (CPIV), CRCoV, canine distemper virus (CDV) and Mycoplasma spp. were performed as previously described (Erles et al., 2004, 2003; Frisk et al., 1999; Kobayashi et al., 1995) on DNA, extracted using the DNeasy Tissue Kit (Qiagen, Crawley) according to the manufacturer's instructions, or on reverse transcribed RNA (Section 2.3).

2.2. Tracheal culture inoculation

For each dog, tracheal culture plates were randomly assigned to a particular inoculation. Tracheal cultures were inoculated after 24 h with CRCoV isolate 4182 (2×10^4 $TCID_{50}$ in 20 μL medium) (Erles et al., 2007), E. coli 055:B5 LPS (10 μg mL^{-1}) (Sigma) or medium only (incl. supplements Section 2.1.1).

2.3. RNA extraction and reverse transcription

Tracheal culture pieces harvested at 24 h intervals were homogenised using a ball mill (Mixer Mill MM 300,

Table 1
Primers for quantitative real-time RT-PCR.

Primer	Sequence (5′–3′)	Nucleotide positions	Product length (bp)
CRCoV *N* gene[a]			
NF3	CCC TAC TAT TCT TGG TTT	8413–8430	140
NR4	CGT CTG TTG TGT CTG TAC C	8552–8534	

[a] CRCoV nucleocapsid gene, NF3 and NR4 (GenBank accession no. DQ682406).

Retsch, Leeds) for 4 min at 20 Hz, and RNA extracted using the RNeasy Mini Kit (Qiagen) following the manufacturer's instructions for RNA extraction from tissue samples. DNase digestion was performed using Turbo DNA-free (Ambion, Huntingdon) according to the manufacturer's instructions. The quantity of RNA was estimated using a NanoDrop-1000 spectrophotometer (Nanodrop Technologies, Wilmington, DE, USA). cDNA synthesis was performed as follows: 1 μg of RNA was added to 1 μg pd(N)$_6$ Random Hexamer (Amersham Biosciences, Little Chalfont) and incubated at 70 °C for 10 min. cDNA was synthesised using the ImProm-II Reverse Transcription System (Promega) according to the manufacturer's instructions.

2.4. CRCoV real-time quantitative RT-PCR

A real-time quantitative RT-PCR for the detection of CRCoV nucleocapsid RNA in tissue samples was developed and the primers are given in Table 1. A plasmid containing the CRCoV nucleocapsid gene target sequence was used to produce a dilution series from 1×10^8 to 1×10^1 copies μL^{-1}. Optimisation of this qPCR is described elsewhere (Mitchell et al., in press).

Quantitative PCR was performed using 12.5 μL of SYBR Green JumpStart *Taq* ReadyMix (Sigma) containing 2.5 mM MgCl$_2$, 10 pmol μL^{-1} of each primer and 1 μL of cDNA or plasmid in a final volume of 25 μL. Amplification was performed in an Opticon 2 real-time thermocycler (Bio-Rad, Hemel Hempstead) and cycling conditions are given in Table 2. cDNA samples and standards were processed in triplicate and a negative control and two internal controls (previously quantified cDNA samples) were included in each PCR series.

2.5. Canine cytokine mRNA quantification

2.5.1. Production of plasmid standards for real-time quantitative RT-PCR

The following cytokines were selected for mRNA quantification in canine tracheal cultures; TNF-α, IL-6 and IL-8. Partial sequences of the canine cytokine genes were amplified by PCR using previously published primers (Peeters et al., 2006; Peters et al., 2005). The template cDNA was obtained by reverse transcription of RNA from canine macrophage-like (DH82) cells stimulated with LPS. The PCR products were cloned into pGEM-T Easy (Promega).

2.5.2. Production of standard curves for cytokine mRNA quantification

Plasmid DNA was quantitated using a NanoDrop-1000 spectrophotometer. The DNA copy number was calculated using the following formula:

$$\text{copies of DNA} = \frac{(\text{concentration}, \mu g\,\mu L^{-1}) \times (6.023 \times 10^{23})}{(\text{DNA size, bp}) \times (660 \times 10^6)}$$

A 10-fold dilution series of each plasmid from 1×10^8 to 1×10^2 copies μL^{-1} was prepared and used as a template to produce a standard curve for assessment of linearity, dynamic range and primer efficiency.

2.5.3. Cytokine mRNA real-time quantitative RT-PCR

The PCR mixture included 12 μL of SYBR Green QPCR Master Mix reagent (Finnzymes, Espoo, Finland), 25 pmol of each primer and 1 μL of DNA in a final volume of 25 μL. The cycling conditions for each cytokine are given in Table 2. cDNA samples and standards were processed in triplicate and a negative control and two internal controls (previously quantified cDNA samples) were included in each PCR series.

Table 2
Real-time quantitative RT-PCR cycling conditions for amplification of canine cytokine mRNAs and CRCoV nucleoprotein RNA.

	Canine TNF-α			Canine IL-6			Canine IL-8			CRCoV nucleoprotein		
	Temp. (°C)	Time	Cycles	Temp. (°C)	Time	Cycles	Temp. (°C)	Time	Cycles	Temp. (°C)	Time	Cycles
Initial denaturation	95	15 min	1	95	15 min	1	95	15 min	1	95	10 min	1
Denaturation	95	10 s	40	95	10 s	40	95	10 s	40	95	10 s	40
Annealing	62.5	15 s		60	15 s		60	15 s		53	20 s	
Extension	72	30 s		72	30 s		72	30 s		72	30 s	
Non-specific product melt	79.5	15 s		80	10 s		75	10 s		79	10 s	
Final annealing	72	5 min	1	72	5 min	1	72	5 min	1	72	5 min	1
Melting curve	70–90	0.2 °C s^{-1}	1	70–90	0.2 °C s^{-1}	1	70–90	0.2 °C s^{-1}	1	65–95	0.2 °C s^{-1}	1
Re-annealing	72	5 min	1	72	5 min	1	72	5 min	1	72	5 min	1

2.5.4. Result analysis and quantification

Results were analysed and quantification performed using standard curves produced by Opticon Monitor software v. 3.1 (Bio-Rad). The absolute copy number of the gene of interest was normalised to cDNA concentration.

Cytokine mRNA copies (ng cDNA^{-1}) were presented as the logarithm of the fold change relative to control-inoculated cultures, from the same dog, at the same time post-inoculation. This method of analysis was adopted to minimise any differences in cytokine mRNA levels due to maintenance of the tracheas *in vitro* and natural variation in baseline levels and responses between different animals. Cytokine mRNA levels were also calculated relative to the CRCoV copy number at a given time point post-inoculation. Statistical analysis of the results of canine cytokine mRNA levels was performed using SPSS v. 16.0 (SPSS Inc., Chicago, USA). The relationship between control- and CRCoV- or LPS-inoculated canine tracheal cultures at a given time was assessed using one-way analysis of variance (ANOVA) and post hoc comparisons made using the Bonferroni method.

2.6. Latex bead clearance assay

10 μL of a suspension of 1 μm diameter latex beads (Polybead polystyrene microsphere beads; Polysciences Europe, Eppelheim, Germany) was pipetted onto the surface of tracheal cultures daily. The beads covered the whole mucosa and following incubation for 30 min each tracheal culture was scored blind by visual inspection according to a scale of 0–5. Zero was defined as no clearance and five was complete clearance of the whole suspension to one edge of the tracheal piece. Statistical analysis of the results of latex clearance was performed using SPSS v. 16.0. The relationship between control- and CRCoV- or LPS-inoculated canine tracheal cultures was assessed using 3-way repeated-measures analysis of variance (RMANOVA) and post hoc comparisons made using the Bonferroni method.

2.7. Immunohistochemistry

Paraffin-embedded formalin-fixed CRCoV-inoculated tracheal culture tissue sections (4 μm) were prepared on SuperFrost Plus microscope slides (Menzel-Gläser, Braunschweig, Germany). Slides were heated at 60 °C for 1 h, deparafinised and rehydrated.

Endogenous peroxidase was blocked with 3% H_2O_2 for 10 min then washed in dH_2O for 5 min. Sections were incubated in pre-warmed (37 °C) protease XIV 0.05% (Sigma) in TBS for 15 min, then rinsed in dH_2O (2 × 2 min). The Shandon Sequenza Coverplate System (Thermo Fisher Scientific, Runcorn) was used to aid slide handling and improve tissue preservation. Sections were incubated with blocking serum (2% normal goat serum [Vector Laboratories, Peterborough] in TBS) then undiluted bovine anti-BCoV polyclonal antiserum conjugated to fluorescein isothiocyanate (FITC) (VMRD Inc., Pullman, WA) overnight at 4 °C.

Sections were washed with blocking serum and incubated with biotinylated goat anti-FITC antibody (1:300 in blocking serum, Vector Laboratories) for 1 h at 37 °C. Sections were washed with blocking serum and incubated with Vectastain Elite ABC Reagent (Vectastain Elite ABC Kit, Vector Laboratories) for 30 min at room temperature, followed by washing in blocking serum. Colour development was carried out using the Vector VIP Substrate Kit (Vector Laboratories) for 8–10 min. Sections were counterstained with Methyl Green (Vector Laboratories) for 4 min, dehydrated and mounted. Positive cells were identified microscopically by the presence of intense purple-brown staining.

3. Results

3.1. Optimisation of quantitative RT-PCR

The majority of cytokine primers had previously been optimised for use with real-time qPCR on canine tissue samples using TaqMan real-time RT-PCR assays (Peeters et al., 2006; Peters et al., 2005). However for each primer set, linearity and efficiency of the PCR were assessed by analysing the correlation coefficient + slope for threshold cycle (C_T) versus log cDNA concentration to ensure the accuracy of mRNA quantification using a SYBR green-based real-time PCR assay.

For each primer set, linearity was confirmed using cDNA obtained from canine tracheal cultures and the plasmid DNA standard curve. High linearity was observed between C_T and the $\log_{10}$ DNA concentration with the correlation coefficient (r) greater than 0.99 for all primer sets used. The slope of the relationship between C_T and the $\log_{10}$ cDNA or plasmid DNA concentration was used to determine the efficiency of the PCR reaction using the following equation:

$$\text{efficiency} = \left(10^{-1/\text{slope}}\right)^{-1}$$

Efficiencies for each qPCR primer set are given in Table 3.

3.2. Canine cytokine mRNA quantification

26 sets of cDNA from tracheal cultures inoculated with CRCoV, LPS or medium-only were available for cytokine mRNA and CRCoV quantification. Levels of TNF-α mRNA in control cultures (medium only) remained constant throughout the time course, however levels of IL-6 and IL-8 mRNA increased from the time of death (−24 h) to a peak at the time of inoculation (0 h) (data not shown). Levels of IL-6 and IL-8 mRNA reduced at each subsequent 24 h of the time course.

Table 3
Efficiency ranges for primer sets used for QPCR.

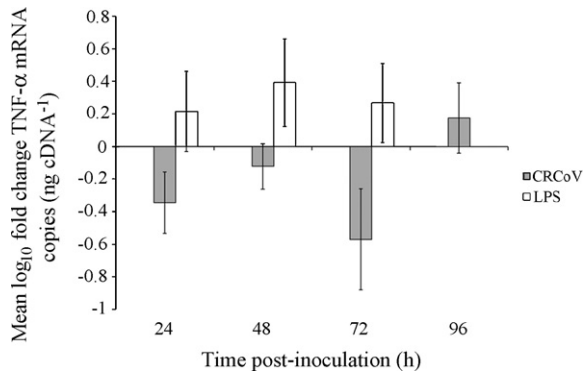| Primer set	Efficiency range
NF3 and NR4	0.76–0.90
CAN TNF-α1 and CAN TNF-α2	0.98–1.03
CAN IL-6F and CAN IL-6R	1.03–1.12
CAN IL-8F and CAN IL-8R	1.01–1.17

Fig. 1. Mean $\log_{10}$ fold change in TNF-α mRNA copies in CRCoV and LPS-inoculated, relative to control-inoculated, tracheal cultures at 24, 48, 72 and 96 h post-inoculation. Error bars show standard error of the mean. No data was available for LPS at 96 h.

TNF-α: canine TNF-α mRNA was quantified over time and the analysis was performed relative to TNF-α mRNA levels in control (medium only) inoculated cultures. LPS-inoculation resulted in an elevation of TNF-α mRNA, relative to controls, at 24, 48 and 72 h post-inoculation, the peak being a 2.5-fold increase, at 48 h post-inoculation (Fig. 1). The TNF-α mRNA levels in CRCoV-inoculated cultures were reduced, relative to controls, at 24, 48 and 72 h. The most marked reduction was observed at 72 h, where cytokine copies were 3.7 times lower than controls; however, at 96 h post-inoculation, TNF-α mRNA copy levels were 1.5 times higher than control-inoculated cultures.

IL-6 and IL-8: LPS inoculation resulted in raised cytokine mRNA copy numbers for both IL-6 and IL-8 and at all three times points (24, 48 and 72 h) post-inoculation (Figs. 2 and 3). mRNA levels of both cytokines were elevated above control levels to the highest degree at 48 h (4.9- and 6.4-fold increase for IL-6 and IL-8, respectively). CRCoV inoculation resulted in the reduction of IL-6 and IL-8 mRNA levels at 24–72 h post-inoculation. For both cytokines, this reduction was greatest at 72 h (6.0- and 5.7-fold decrease for IL-6 and IL-8, respectively). IL-6 and IL-8 mRNA levels were increased compared to controls at 96 h.
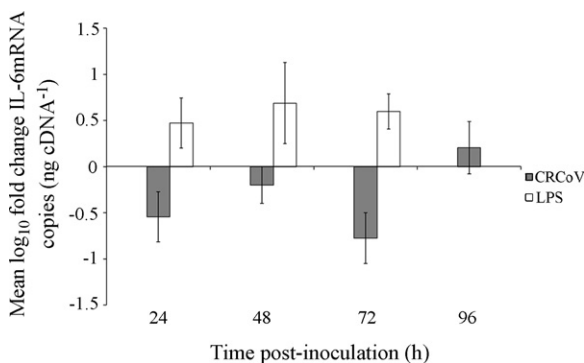
There was no significance difference ($p > 0.05$) between measured cytokine mRNA levels in control or CRCoV-inoculated cultures at any time point. Significant differences were obtained for LPS inoculation at 24, 48 and 72 h ($p = 0.01$).

3.3. CRCoV nucleocapsid gene RNA quantification

The development of an accurate method for the quantification of CRCoV in tissue samples enabled nucleocapsid gene RNA to be quantified in cDNA from canine tracheal cultures inoculated with CRCoV. The mean CRCoV nucleocapsid gene copy number within tracheal cultures from different dogs at 24–96 h post-inoculation was determined (Fig. 4). In all cases, there was an overall increase in CRCoV nucleocapsid gene RNA copies during the experiment and the peak copy number was attained at 96 h post-inoculation for each dog. However, in some dogs, there was a noticeable fall in copy number at 48 or 72 h, compared to the levels at 24 h, thus the dynamics of the infection appeared to be different for tracheal cultures from different dogs. Due to this finding, cytokine mRNA levels were also analysed relative to CRCoV copy number, to control for individual variation between the tracheas

Fig. 3. Mean $\log_{10}$ fold change in IL-8 mRNA copies in CRCoV and LPS-inoculated, relative to control-inoculated tracheal cultures at 24, 48, 72 and 96 h post-inoculation. Error bars show standard error of the mean. No data was available for LPS at 96 h.
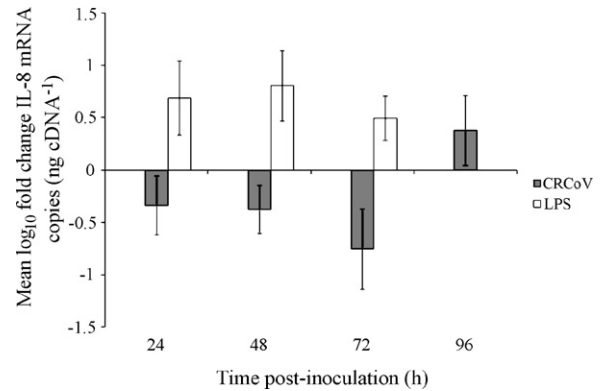

Fig. 2. Mean $\log_{10}$ fold change in IL-6 mRNA copies in CRCoV and LPS-inoculated, relative to control-inoculated tracheal cultures at 24, 48, 72 and 96 h post-inoculation. Error bars show standard error of the mean. No data was available for LPS at 96 h.
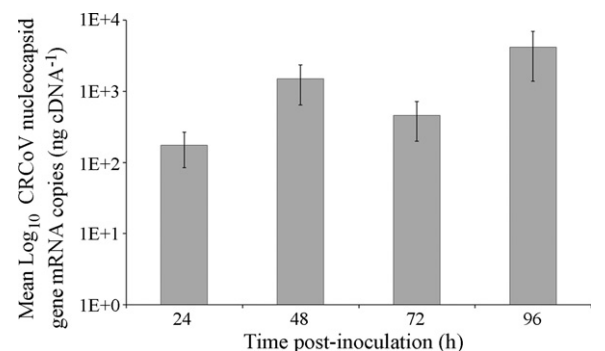

Fig. 4. Mean CRCoV nucleocapsid gene RNA copies (ng cDNA^{-1}) in canine tracheal cultures at 24, 48, 72 and 96 h post-inoculation with CRCoV. Error bars show standard error of the mean.
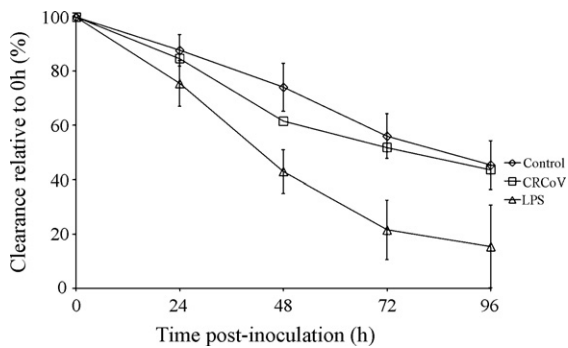
Fig. 5. Tracheal culture latex clearance scores after 30 min at 24 h intervals, given as a percentage of the maximal clearance of each tracheal piece recorded pre-inoculation (0 h) and recorded over 96 h. Error bars show standard error of the mean.

from different dogs. The quantification of canine IL-6, IL-8 and TNF-α mRNA copies in CRCoV-inoculated cultures was presented as the logarithm of the fold change relative to control-inoculated cultures in the same dog at the same time point. These data were plotted against CRCoV nucleocapsid RNA copies in the same cDNA sample. The Pearson correlation coefficient, r was determined for each cytokine using SPSS v. 16.0. There were weak positive correlations between the fold change in IL-6 ($r = 0.304$) and IL-8 ($r = 0.277$) mRNA copies and CRCoV copies, however these were not considered significant ($p > 0.05$). A significant positive correlation ($p = 0.05$) was demonstrated between TNF-α mRNA and CRCoV RNA copies ($r = 0.382$). Interestingly at low CRCoV RNA copy number (below 2.0 logs), cytokine mRNA copies appeared to be reduced relative to controls.

3.4. Latex clearance assay

The mean maximal clearance score, based on four individual cultures (selected arbitrarily from different areas of the trachea to reduce the effects of any potential intra-tracheal variation in ciliary function), was obtained after 30 min incubation immediately prior to inoculation (0 h) and was regarded as 100%. The mean clearance scores at each subsequent 24 h interval, up to 120 h post-mortem, were calculated as a percentage relative to the original clearance score thus giving an overall score for each condition, at each time point, per dog. Assessment relative to the initial clearance was used to negate the inherent variation in ciliary function between different tracheas.

A gradual reduction in latex clearance score was observed for all inoculation conditions, including the control, over 96 h (Fig. 5). After 96 h, LPS-inoculated cultures retained only 15.3% of their initial clearance at 0 h and had average latex clearance scores of 30% less than the medium only controls. CRCoV-inoculated cultures had 43.6% of the initial clearance remaining after 96 h, compared with 45.3% for control-inoculated cultures. CRCoV-inoculated cultures had the greatest differential from controls at 48 h (12.6%), however by 96 h, the rate in decline of clearance score had slowed and essentially mirrored the control.

Ciliary clearance was found to be significantly different between control- and LPS-inoculated cultures for the time period 24–96 h post-inoculation ($p = 0.002$). However, no significant difference ($p > 0.05$) was found between control- and CRCoV-inoculated cultures in ciliary latex clearance over the same period post-inoculation.

Assessment of latex clearance at 10 min intervals was used to try to detect more subtle changes in ciliary function, more specifically an altered rate of latex clearance (data not shown). Ciliary clearance was found to be significantly different between control- and LPS-inoculated cultures for the time period 10–60 min post-inoculation ($p = 0.0001$). However, no significant difference ($p > 0.05$) was found between control- and CRCoV-inoculated cultures, over the same period.

3.5. Immunohistochemistry

Coronaviral-antigen positive cells were detected within the epithelium of CRCoV-inoculated tracheal culture sections (Fig. 6). Positive staining was present in the cytoplasm of ciliated columnar epithelial and goblet cells. The distribution of positive cells was relatively scant, but widespread, often occurring as small groups of positive cells. Aggregates of positively stained material were observed on the luminal surface of the trachea and these were invariably located adjacent to coronaviral-antigen positive cells. Less frequently, coronaviral-antigen positive cells were surrounded by areas of vacuolation within the epithelium, possibly representing a cytopathic effect of the virus.

Tracheas from naturally infected CIRD cases, where CRCoV was detected by RT-PCR, were also examined (Fig. 6). Intra-cytoplasmic staining of epithelial cells within the trachea of naturally infected dogs was in agreement with that observed in the CRCoV-inoculated cultures.

4. Discussion

In vitro models, particularly those involving the respiratory system, must be physiologically relevant and closely match the *in vivo* environment for the accurate modelling of viral pathogenesis. Many cell culture-adapted cell lines have either lost the ability to synthesize and secrete certain cytokines or else their responses to stimuli, such as viruses, are altered by growth in culture. The relevance of using isolated cell populations, removed from their normal context, for the study of the complex multicellular interactions of viruses *in vivo* is therefore greatly reduced.

The global distribution and high seroprevalence of CRCoV suggest a virus that is contagious but has the ability to spread through canine populations, for the most part, clinically undetected. To appreciate further the role of CRCoV in canine respiratory disease, an *in vitro* model of the hypothesised main target tissue, the trachea, was developed. This study represents the first use of an organ culture system, incorporating an air-interface, in assessment of the functional consequences of virus replication in dogs.

Knowledge of the epithelial immune response is crucial for the further understanding of CRCoV pathogenesis. The
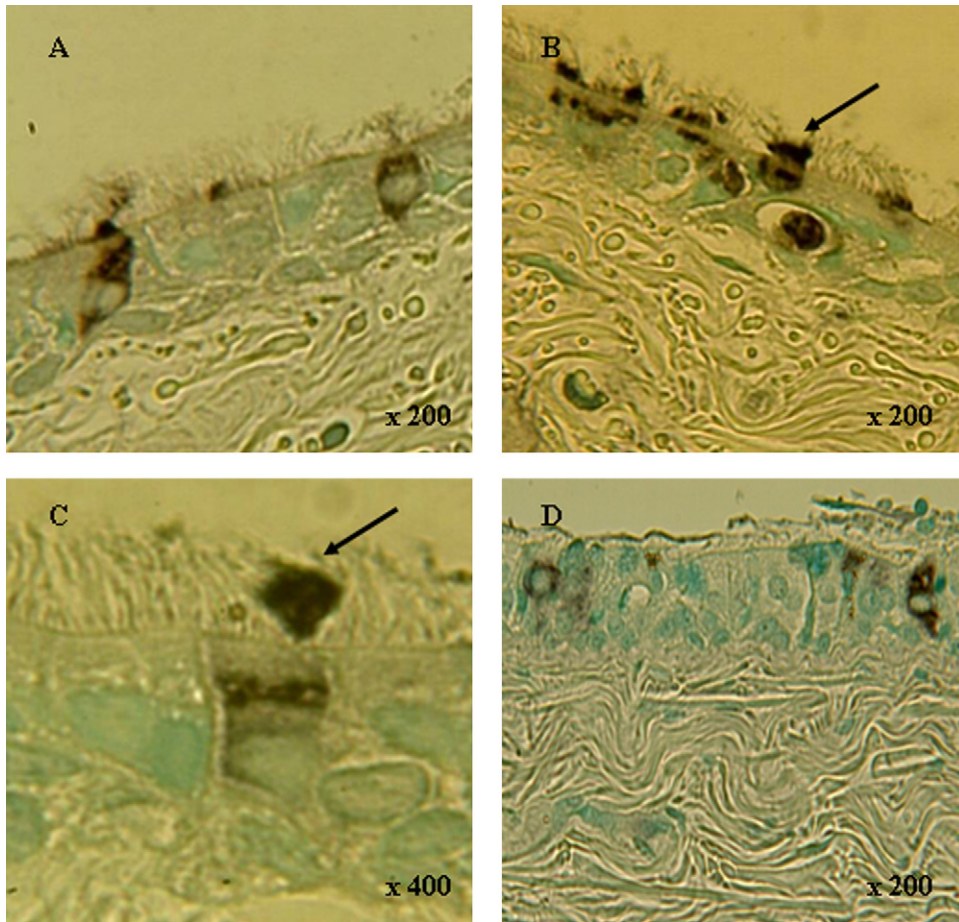
Fig. 6. Immunohistochemical staining of CRCoV-inoculated canine tracheal cultures (A–C) and naturally infected canine trachea, positive for CRCoV by RT-PCR (D). (A–D) Trachea—coronaviral-antigen positive epithelial cells and corresponding surface/ciliary layer antigen accumulation (arrows). Chromogen, Vector VIP; counterstain, methyl green.

mRNA levels of pro-inflammatory cytokines and chemokines were therefore quantified following CRCoV inoculation. LPS was chosen as a positive control as this has previously been shown to be a potent inducer of innate immunity and the corresponding cytokine profile in humans (Boeuf et al., 2005) and significantly decreased ciliary activity in rat tracheal organ cultures (Johnson and Inzana, 1986).

The cytokines selected for investigation in this study were chosen based on their involvement in other coronavirus infections. In response to LPS, mRNA levels of TNF-α, IL-6 and IL-8 in cultures, were significantly increased from 24 h post-inoculation, relative to controls, indicating that the assay was sensitive enough to detect changes in cytokine mRNAs within this system. Peak levels for all three cytokine mRNAs were detected at 48 h and had declined by 72 h. Interestingly, CRCoV appeared to suppress the mRNA levels of pro-inflammatory cytokines from 24 to 72 h post-inoculation, however at 96 h the levels were raised for each cytokine. When correlated with actual copies of virus, it appeared that at lower copy number (as would be present during the earlier part of the time-course), there was active suppression of cytokine mRNA, relative to controls. How-ever, it seemed that once the virus copies reached a threshold, of 100 copies ng cDNA^{-1}, cytokine mRNA levels were increased relative to controls, as recorded at 96 h. It is conceivable that early non-structural proteins produced by the replicating virus may act to inhibit the induction of cytokine and chemokine genes. Down-regulation of IFN-responses by non-structural proteins is a strategy many viruses have evolved to remain successful pathogens (Haller et al., 2006).

Recently BCoV has been shown not to induce a detectable pro-inflammatory response in calf intestine following inoculation (Aich et al., 2007). Quantitative RT-PCR analysis of IL-6 and TNF-α genes revealed that both were down-regulated following BCoV infection and the authors concluded that the absence of a pro-inflammatory response may result in a more prolonged infection.

SARS-CoV is highly sensitive to the antiviral actions of IFNs, both in vitro and in vivo which may explain why the virus has been shown to actively suppress the activation of antiviral and IFN-induced effector genes via the inhibition of the crucial cytokine transcription factor, IRF3 (Spiegel et al., 2005; Spiegel and Weber, 2006). The suppression of the immediate early interferon response, via the absence of

IRF3, is now thought to be a feature of all group 2 coronaviruses (Versteeg et al., 2007). The suppression of antiviral cytokines in non-immune cells by SARS-CoV is thought to buy time for dissemination of the virus in the host and a similar mechanism may be employed by CRCoV.

All cultures, including controls, were subject to gradual tissue degeneration. The upregulation of pro-inflammatory cytokines would be a normal tissue response to such injury. Cytokine gene expression levels in human tonsil *ex vivo* cultures were similar to the levels at the time of excision, except IL-6 and IL-8 which were markedly increased following the first 24 h of culture hypothesised to be due to initial stress of culture (Bonanomi et al., 2003). In the current model the same pattern was observed for IL-6 and IL-8 mRNA in control cultures, whereas TNF-α mRNA levels remained stable. In control-inoculated cultures increased cytokine mRNA levels may have occurred as a response to maintenance in culture. The reduction in cytokine mRNA in CRCoV-inoculated cultures, relative to controls, may have been due to CRCoV actively inhibiting pro-inflammatory responses through an as yet unknown mechanism. Increased cytokine mRNAs were observed at 96 h in CRCoV-inoculated cultures. The replication of CRCoV within the cultures may have progressed more slowly than anticipated and had the cultures been maintained for longer than 96 h, possible further increases in cytokines might have been observed.

The use of an accurate method for the quantification of CRCoV in canine tissue samples was extremely useful in this study. Whilst the assay could not differentiate between live virus and simply genetic material from non-viable particles, steps were taken to minimise this risk. The washing of tracheal pieces prior to the extraction of RNA meant that only virus internalised within cells would be quantified. The assay demonstrated that the growth kinetics of CRCoV within this system were not linear. Despite the application of a uniform virus inoculum, differences in ciliary function and the thickness and nature of the mucus layer between dogs may have resulted in variation in the physical barrier to virus receptor binding and penetration of epithelial cells. Cultures from all dogs included in this study were subject to an increase in overall CRCoV nucleoprotein gene RNA copies by 96 h post-inoculation, indicating that viral replication was occurring. The differences between individual tracheal cultures were representative of the heterogeneous *in vivo* situation and variation between dogs was minimised by the use of control-inoculated cultures, which acted as a baseline for the responses of individual tracheas.

The presence of ciliary clearance is a key strategy for the removal of pathogens from the respiratory tree and ciliary loss is a known consequence of immersion of cultures in medium. A deficient ciliary clearance mechanism in the trachea would potentiate the invasion and colonisation of more serious respiratory pathogens such as *Bordetella bronchiseptica*. Cultures were shown to retain co-ordinated ciliary beating for up to 144 h post-mortem in this system. Ciliary function declined between the time of death and culture inoculation. However, following inoculation, the ciliary clearance of LPS-inoculated cultures was significantly reduced with respect to both the speed and extent of clearance of latex relative to controls. Whilst the effects of CRCoV on ciliary function were not found to be significantly different to controls, CRCoV was capable of limiting the ciliary function of canine tracheal epithelium at 48 h post-inoculation. Between 72 and 96 h, the ciliary clearance of CRCoV-inoculated cultures was similar to that of controls, suggesting that any effects of CRCoV on the respiratory epithelium happen early in the course of infection.

The CRCoV isolate used in the inoculation of tracheal cultures had been adapted to growth in a human rectal adenocarcinoma cell line (HRT-18 cells) (Erles et al., 2007) and the challenge dose of virus was the maximum titre to which CRCoV could be cultured. The functional responses observed following virus challenge may be limited as a consequence of a loss of virulence or replicative efficiency within canine respiratory cells.

IHC revealed coronavirus antigen positive intra-cytoplasmic staining of ciliated epithelial and goblet cells within canine tracheas of both CRCoV-inoculated cultures and from naturally infected cases of CIRD. Whilst the number of coronaviral-antigen positive cells was greater in experimentally inoculated tissue, the same cell types and distribution were observed in naturally infected tracheal tissue. These findings were in agreement with previous work which identified coronaviral-antigen positive epithelial cells within the bronchi and major bronchioles of two cases of CIRD (Ellis et al., 2005). The greatest accumulations of antigen-positive material were located on the apical aspect of cells and often in association with luminal aggregations overlying the tracheal surface, possibly representing secreted antigen, retained on the surface in the periciliary mucus layer. The distribution of CRCoV in the canine trachea mirrors that of BCoV in bovine tissues, where the primary sites of infection are the epithelial cells of the nasal cavity and trachea, leading to mild upper respiratory signs such as coughing, sneezing and rhinitis (Reynolds et al., 1985).

The effects of CRCoV on the mucociliary and innate immune systems were observed within 24 h of inoculation. A moderate reduction in ciliary function may be due to cellular damage during viral replication. During this time mucociliary compromise and down-regulation of pro-inflammatory cytokines by CRCoV may present a 'window' of opportunity for the entry of other viral or bacterial pathogens, thus potentiating more serious respiratory disease. On its own, CRCoV may cause a transient potentially clinically silent, respiratory disease similar to the human 'common cold'. However, challenge with CRCoV during entry to a re-homing kennel is often accompanied by the simultaneous exposure to CPIV, CHV, *B. bronchiseptica* and mycoplasmas, in addition to the environmental stresses that are inevitable during such an event. The simultaneous or sequential actions of these agents, primed by CRCoV, could lead to the development of CIRD and potentially outbreak situations.

Acknowledgements

would like to thank Sandra Greaves for technical assistance.

References

Adachi, M., Matsukura, S., Tokunaga, H., Kokubu, F., 1997. Expression of cytokines on human bronchial epithelial cells induced by influenza virus A. Int. Arch. Allergy Immunol. 113, 307–311.

Adler, K.B., Fischer, B.M., Wright, D.T., Cohn, L.A., Becker, S., 1994. Interactions between respiratory epithelial cells and cytokines: relationships to lung inflammation. Ann. N Y Acad. Sci. 725, 128–145.

Aich, P., Wilson, H.L., Kaushik, R.S., Potter, A.A., Babiuk, L.A., Griebel, P., 2007. Comparative analysis of innate immune responses following infection of newborn calves with bovine rotavirus and bovine coronavirus. J. Gen. Virol. 88, 2749–2761.

Anderton, T.L., Maskell, D.J., Preston, A., 2004. Ciliostasis is a key early event during colonization of canine tracheal tissue by Bordetella bronchiseptica. Microbiology 150, 2843–2855.

Becker, S., Koren, H.S., Henke, D.C., 1993. Interleukin-8 expression in normal nasal epithelium and its modulation by infection with respiratory syncytial virus and cytokines tumor necrosis factor, interleukin-1, and interleukin-6. Am. J. Respir. Cell. Mol. Biol. 8, 20–27.

Boeuf, P., Vigan-Womas, I., Jublot, D., Loizon, S., Barale, J.C., Akanmori, B.D., Mercereau-Puijalon, O., Behr, C., 2005. CyProQuant-PCR: a real time RT-PCR technique for profiling human cytokines, based on external RNA standards, readily automatable for clinical use. BMC Immunol. 6, 5.

Bonanomi, A., Kojic, D., Giger, B., Rickenbach, Z., Jean-Richard-Dit-Bressel, L., Berger, C., Niggli, F.K., Nadal, D., 2003. Quantitative cytokine gene expression in human tonsils at excision and during histoculture assessed by standardized and calibrated real-time PCR and novel data processing. J. Immunol. Methods 283, 27–43.

Brydon, E.W., Morris, S.J., Sweet, C., 2005. Role of apoptosis and cytokines in influenza virus morbidity. FEMS Microbiol. Rev. 29, 837–850.

Decaro, N., Desario, C., Elia, G., Mari, V., Lucente, M.S., Cordioli, P., Colaianni, M.L., Martella, V., Buonavoglia, C., 2007. Serological and molecular evidence that canine respiratory coronavirus is circulating in Italy. Vet. Microbiol. 121, 225–230.

Ellis, J.A., McLean, N., Hupaelo, R., Haines, D.M., 2005. Detection of coronavirus in cases of tracheobronchitis in dogs: a retrospective study from 1971 to 2003. Can. Vet. J. 46, 447–448.

Erles, K., Dubovi, E.J., Brooks, H.W., Brownlie, J., 2004. Longitudinal study of viruses associated with canine infectious respiratory disease. J. Clin. Microbiol. 42, 4524–4529.

Erles, K., Shiu, K.B., Brownlie, J., 2007. Isolation and sequence analysis of canine respiratory coronavirus. Virus Res. 124, 78–87.

Erles, K., Toomey, C., Brooks, H.W., Brownlie, J., 2003. Detection of a group 2 coronavirus in dogs with canine infectious respiratory disease. Virology 310, 216–223.

Frisk, A.L., Konig, M., Moritz, A., Baumgartner, W., 1999. Detection of canine distemper virus nucleoprotein RNA by reverse transcription-PCR using serum, whole blood, and cerebrospinal fluid from dogs with distemper. J. Clin. Microbiol. 37, 3634–3643.

Haller, O., Kochs, G., Weber, F., 2006. The interferon response circuit: induction and suppression by pathogenic viruses. Virology 344, 119–130.

Jackson, A.D., Rayner, C.F., Dewar, A., Cole, P.J., Wilson, R., 1996. A human respiratory-tissue organ culture incorporating an air interface. Am. J. Respir. Crit. Care Med. 153, 1130–1135.

Jang, Y.J., Lee, S.H., Kwon, H.J., Chung, Y.S., Lee, B.J., 2005. Development of rhinovirus study model using organ culture of turbinate mucosa. J. Virol. Methods 125, 41–47.

Johnson, A.P., Inzana, T.J., 1986. Loss of ciliary activity in organ cultures of rat trachea treated with lipo-oligosaccharide from Haemophilus influenzae. J. Med. Microbiol. 22, 265–268.

Johnson, L.R., Maggs, D.J., 2005. Feline herpesvirus type-1 transcription is associated with increased nasal cytokine gene transcription in cats. Vet. Microbiol. 108, 225–233.

Kaneshima, T., Hohdatsu, T., Satoh, K., Takano, T., Motokawa, K., Koyama, H., 2006. The prevalence of a group 2 coronavirus in dogs in Japan. J. Vet. Med. Sci. 68, 21–25.

Kazachkov, M.Y., Hu, P.C., Carson, J.L., Murphy, P.C., Henderson, F.W., Noah, T.L., 2002. Release of cytokines by human nasal epithelial cells and peripheral blood mononuclear cells infected with Mycoplasma pneumoniae. Exp. Biol. Med. (Maywood) 227, 330–335.

Kobayashi, H., Yamamoto, K., Eguchi, M., Kubo, M., Nakagami, S., Wakisaka, S., Kaizuka, M., Ishii, H., 1995. Rapid detection of mycoplasma contamination in cell cultures by enzymatic detection of polymerase chain reaction (PCR) products. J. Vet. Med. Sci. 57, 769–771.

Okabayashi, T., Kariwa, H., Yokota, S., Iki, S., Indoh, T., Yokosawa, N., Takashima, I., Tsutsumi, H., Fujii, N., 2006. Cytokine regulation in SARS coronavirus infection compared to other respiratory virus infections. J. Med. Virol. 78, 417–424.

Peeters, D., Peters, I.R., Clercx, C., Day, M.J., 2006. Real-time RT-PCR quantification of mRNA encoding cytokines, CC chemokines and CCR3 in bronchial biopsies from dogs with eosinophilic bronchopneumopathy. Vet. Immunol. Immunopathol. 110, 65–77.

Peters, I.R., Helps, C.R., Calvert, E.L., Hall, E.J., Day, M.J., 2005. Cytokine mRNA quantification in histologically normal canine duodenal mucosa by real-time RT-PCR. Vet. Immunol. Immunopathol. 103, 101–111.

Priestnall, S.L., Brownlie, J., Dubovi, E.J., Erles, K., 2006. Serological prevalence of canine respiratory coronavirus. Vet. Microbiol. 115, 43–53.

Priestnall, S.L., Pratelli, A., Brownlie, J., Erles, K., 2007. Serological prevalence of canine respiratory coronavirus in southern Italy and epidemiological relationship with canine enteric coronavirus. J. Vet. Diagn. Invest. 19, 176–180.

Reynolds, D.J., Debney, T.G., Hall, G.A., Thomas, L.H., Parsons, K.R., 1985. Studies on the relationship between coronaviruses from the intestinal and respiratory tracts of calves. Arch. Virol. 85, 71–83.

Spiegel, M., Pichlmair, A., Martinez-Sobrido, L., Cros, J., Garcia-Sastre, A., Haller, O., Weber, F., 2005. Inhibition of beta interferon induction by severe acute respiratory syndrome coronavirus suggests a two-step model for activation of interferon regulatory factor 3. J. Virol. 79, 2079–2086.

Spiegel, M., Weber, F., 2006. Inhibition of cytokine gene expression and induction of chemokine genes in non-lymphatic cells infected with SARS coronavirus. Virol. J. 3, 17.

Versteeg, G.A., Bredenbeek, P.J., van den Worm, S.H., Spaan, W.J., 2007. Group 2 coronaviruses prevent immediate early interferon induction by protection of viral RNA from host cell recognition. Virology 361, 18–26.